# Longitudinal assessment of PD-L1 expression and gene expression profiles in patients with head and neck cancer reveals temporal heterogeneity

Andy Karabajakian, Jebrane Bouaoud, Lucas Michon, Maud Kamal, Carole Crozes, Philippe Zrounba, Jessie Auclair-Perossier, Nicolas Gadot, Valéry Attignon, Christophe Le Tourneau, et al.

# Longitudinal assessment of PD-L1 expression and gene expression profiles in patients with head and neck cancer reveals temporal heterogeneity

Andy Karabajakian[1, 2] *, Jebrane Bouaoud[2, 3]*, Lucas Michon[2], Maud Kamal[4], Carole Crozes[5], Philippe Zrounba[6], Jessie Auclair-Perossier[2], Nicolas Gadot[2], Valéry Attignon[2], Christophe Le Tourneau[4], Nazim Benzerdjeb[7, 8], Jérôme Fayette[1], Pierre Saintigny[1, 2]

[1]Department of Medical Oncology, Centre Léon Bérard, Lyon, France. [2]Univ Lyon, Université Claude Bernard Lyon 1, INSERM 1052, CNRS 5286, Centre Léon Bérard, Centre de Recherche en Cancérologie de Lyon, Lyon 69008, France, [3]Sorbonne Université, Department of Maxillo-Facial Surgery, Hôpital Pitié-Salpêtrière, Assistance Publique des Hôpitaux de Paris, Paris, France. [4]Department of Drug Development (D3i), INSERM U900 Research unit, Institut Curie, Paris-Saclay University, Paris & Saint-Cloud [5]Department of pathology, Centre Léon Bérard, Lyon, France. [6]Department of Surgical Oncology, Centre Léon Bérard, Lyon, France. [7]Department of Pathology, Institut de Pathologie Multisite, Groupement Hospitalier Sud, Hospices Civils de Lyon, Pierre-Bénite, France. [8]EA 37.38 - Centre d'Innovation en Cancérologie de Lyon (CICLy), Université Claude Bernard Lyon 1, Faculté de médecine Lyon-Sud, Oullins, France.

* These authors contributed equally to this work

**Corresponding author:** Pierre Saintigny, M.D., Ph.D., Department of Medical Oncology, Centre Léon Bérard, 28 Promenade Léa et Napoléon Bullukian, 69008 Lyon, France; Email: pierre.saintigny@lyon.unicancer.fr

**Funding/Support :** ITMO Cancer 2020, Formation à la Recherche Fondamentale et Translationnelle en Cancérologie (JB) ; Bristol-Myers Squibb Foundation (PS and JF); Ligue contre le Cancer 2020 (JB and PS) and 2017-INCa-DGOS-Inserm_12563 Integrated Site for Cancer Research (SIRIC): LYriCAN.

**Word count:** 2,166

**Abstract (226 words)**

**Background:** Programmed death-ligand 1 (PD-L1) is the most validated predictive biomarker used for the treatment of head and neck squamous cell carcinoma (HNSCC) with immune checkpoint inhibitors (ICI). Several gene expression-based signatures surrogate of the activation of IFN-gamma pathway and of the presence of tertiary lymphoid structures (TLS) have also been proposed as potential biomarkers. While they may have a potential therapeutic implication, the longitudinal changes of either PD-L1 or gene expression profiles between the initial and recurrent HNSCC lesions is unknown.

**Methods:** PD-L1 immunohistochemistry (IHC) and targeted RNA-sequencing of 2,549 transcripts were analyzed on paired specimens from the initial diagnosis and recurrent HNSCC. PD-L1 status was defined using the combined positive score (CPS). PD-L1 mRNA levels were compared with protein expression levels by IHC. Enrichment scores of surrogate signatures for TLS and IFN-gamma (IFN-γ) pathway activation were computed using the single sample gene set enrichment analysis (ssGSEA).

**Results:** PD-L1 status was 64% (21/33) concordant between the initial and recurrent lesions using a CPS 1 threshold and 67% (22/33) concordant using a CPS 20 threshold. CPS score was associated with PD-L1 gene expression levels. There was a 43% (15/35) and 66% (23/35) concordance for the IFN-γ and TLS signature scores, respectively.

**Conclusion:** Our study reveals temporal heterogeneity of PD-L1 status and TLS/IFN-γ gene expression surrogates in HNSCC that need to be considered when interpreting biomarker studies.

**Key words:** Programmed Death Ligand 1, Transcriptome, Squamous Cell Carcinoma of Head and Neck, Gene expression.

**Abbreviation List**

**APC:** antigen-presenting cells

**CPS:** combined positive score

**CTLA4:** cytotoxic T-lymphocyte antigen 4

**FFPE:** formalin-fixed, paraffin-embedded

**GEP:** gene expression profiles

**GSEA:** gene set enrichment analysis

**HNSCC:** head & neck squamous cell carcinoma

**HPV:** human-papillomavirus

**ICI:** immune checkpoint inhibitors

**IFN-γ:** interferon-gamma

**KIR:** killer immunoglobulin-like receptor

**OS:** overall survival

**OSCC:** oral squamous cell carcinoma

**PD-L1:** programmed death-ligand 1

**PFS:** progression-free survival

**RECIST:** Response Evaluation Criteria in Solid Tumors

**R/M:** recurrent/metastatic

**ssGSEA:** single sample gene set enrichment analysis

**SS:** surgical specimens.

**TB:** tumor biopsy

**TLS:** tertiary lymphoid structures

## 1. Background

Head and neck squamous cell carcinoma (HNSCC) is the sixth most incident cancer worldwide [1]. Despite aggressive multimodal therapeutic approaches including surgical resection (often with neck dissection), radiation therapy and adjuvant chemotherapy, more than half of the patients with locally advanced disease experience locoregional or distant relapse not amenable to curative treatments [2].

Since the dawn of immunotherapy with checkpoint blockade and its establishment in HNSCC as a therapeutic standard in the incurable recurrent and/or metastatic (R/M) setting [3-6], major efforts have been deployed towards the development of robust predictive biomarkers [7], considering the high cost of this treatment, its toxicity profile and reports of induced disease acceleration, or "hyperprogressive" disease (HPD) [9-10]. Programmed death-ligand 1 (PD-L1) protein expression by immunohistochemistry (IHC) has been shown to be partially correlated with response to immune checkpoint inhibitors (ICI) in HNSCC but complete responses have been observed in PD-L1-negative patients [3-6]. The FDA approved pembrolizumab for use in combination with platinum and fluorouracil for all patients and as a single agent for patients with a CPS [(Combined Positive Score), which is the number of PD-L1 staining cells (tumor cells, lymphocytes, macrophages) divided by the total viable tumor cells, multiplied by 100) ] $\geq$ 1. Nivolumab is approved for patients progressing after a first-line platinum-based therapy, after showing a 32% reduction in the risk of death in the Checkmate 141 trial [2,3].

The value of PD-L1 expression by IHC as a predictive biomarker is undermined for several reasons which might explain the discordant results seen across studies. Beyond assays and cut-off diversity [11], an important reason for observed discordant results may be the spatial and temporal heterogeneity of PD-L1 expression. Indeed, its expression, often assessed from single tumor biopsies, varies within a given tumor [12]. A Danish team prospectively investigated intratumor heterogeneity of PD-L1 expression in HNSCC using six random core biopsies from each unique surgical specimen to assess the concordance between multiple biopsies [13]. Concordance was as low as 36 to 70%, depending on the positivity cut-offs used for evaluation.

PD-L1 expression may also change during the course of the disease from the initial diagnosis to the time of disease progression as previously reported in other tumor types [14,15]. Longitudinal PD-L1 expression changes in HNSCC is poorly described and may impact its value as a predictive biomarker.

Other predictive biomarkers of response to ICI have been proposed including tumor mutational burden [16], intratumoral immune cell infiltration [17] and gene expression profiles (GEP) [18]. However, they have not yet been validated in prospective clinical trials. In this search for biomarkers, efforts to identify a pancancer GEP resulted in the elaboration of a number of gene signatures, including in HNSCC [19].

The role of interferon-gamma (IFN-γ) signaling as an inducer of PD-L1 expression [20,21] has led to several IFN-γ/T-cell-inflamed signatures that were shown to correlate with response to ICI [22,23], including in HNSCC [24,25].

Tertiary lymphoid structures (TLS) are cellular aggregates that can be present in tumors and be the site of

antitumoral defense, with a structural organization resembling that of secondary lymphoid organs [26]. They contain activated and proliferating effector T-cells and memory B-cells, along with antigen-presenting cells (APC) [26]. For this reason, recent data has emerged regarding their value as a predictive biomarker of response to ICI [27,28]. As such, various gene expression-based signatures reflecting the presence of TLS have been proposed, related to the presence of chemokines [29,30] or specific cell populations known to play a major role in the formation of TLS [31,32].

Very little is known on the longitudinal changes of both TLS and IFN-γ/T-cell-inflamed gene expression-based signatures in sequential biopsies of patients with HNSCC.

In this work, we assessed PD-L1 protein and gene expression as well as GEP surrogates of IFN-γ and TLS in patients with HNSCC using paired tumor biospecimens from the same patients to get more insight into their longitudinal changes.

## 2. Material and methods

### Patient selection and data collection

The study was approved by the Institutional review board and done in accordance with the Helsinki Declaration. All patients with a histologically confirmed R/M HNSCC treated at Centre Léon Bérard (Lyon, France) and Institut Curie (Paris, France) in a clinical trial evaluating an anti-PD-1/PD-L1 antibody alone or in combination with an anti-cytotoxic T-lymphocyte antigen 4 (CTLA4) or an anti-killer immunoglobulin-like receptor (KIR) between March 2014 and November 2018 were examined. Those with at least two available formalin-fixed, paraffin-embedded (FFPE) tumor samples were included in this study. For a given patient, each specimen was sampled in a different disease stage (initial diagnosis and recurrence stage). In case of neoadjuvant chemotherapy, analysis of the initial diagnosis setting was performed on a sample provided before any systemic treatment. Collection of data and analysis was in accordance with guidelines of each of these trials. The following data were collected and recorded: gender, age, primary tumor location, smoking history, HPV status (p16 immunostaining and/or DNA in situ hybridization) and previous multimodal therapy at the initial stage.

The data collection cutoff date was September 15, 2020.

### Immunohistochemistry

4-µm thick FFPE tissue sections were prepared according to conventional procedures. For each sample, hematoxylin and eosin staining was performed to determine the percentage of tumor cells. IHC was performed on an automated immunostainer (Ventana Benchmark ultra, Roche, Meylan, France) using Ultra View DAB Kit according to the manufacturer's instructions. Sections were incubated with a rabbit monoclonal human anti-PD-L1 antibody (diluted at 1:50, Quartett, Berlin, Germany) clone QR1. The Ventana amplification kit was used and an anti-rabbit-HRP was applied on sections. Staining was visualized with DAB solution with 3,3′-diaminobenzidine as a chromogenic substrate. Finally, the sections were counterstained with Gill's hematoxylin. All samples were examined by two qualified anatomopathologists

(C.C and N.B) for determination of the CPS, defined as the number of PD-L1-positive cells (tumor cells, macrophages and lymphocytes) divided by the number of viable tumor cells × 100 (a minimum of 100 viable tumor cells must have been present for the specimen to be considered evaluable) (Supplementary Figure S1 and S2). In case of inter-observer disagreement over the CPS, a supplementary review of the slides was performed simultaneously by the two pathologists for a final scoring.

In a previous publication, the authors have compared the correlation and concordance of the QR1 and the standard 22C3 antibodies by testing on 110 lung adenocarcinomas. They have found a strong correlation (r=0.82) and concordance for the different thresholds between the two antibodies [33]. The QR1 antibody has received the CE-IVD (Conformité Européenne marking for In Vitro Diagnostic) designation in Europe [34]. For internal validation, we performed a blinded analysis of the QR1 and 22C3 antibodies on 17 samples, showing a high concordance (14/17, 82%) (Table S1).

**Gene expression profiling**

GEP were generated by targeted-RNA sequencing in FFPE samples using the HTG EdgeSeq technology [35] and the Oncology Biomarker Panel (OBP) (2,559 transcripts). For a given patient, GEP were generated on the initial diagnostic tissue sample (surgically resected specimen or per-endoscopic biopsy) and on a new biopsy sampled at the time of disease recurrence. Probe and assay design, sample preparation, nuclease protection assay, PCR tagging and library cleanup are detailed in supplementary material and methods. Sequencing was performed on an Illumina NextSeq instrument. Sequencing libraries were loaded with a 5% PhiX spike-in. Standard Illumina protocols were used for library denaturation. 50 cycles of sequencing were performed with two 6-base barcode reads. The sequencer performed demultiplexing and fastq files were returned. The HTG EdgeSeq parser was used to align the probe sequences to the results; this program is a front end for bowtie2 software, using a 25-base match with one mismatch allowed to the first 25 bases of sequencing information. The final data table is a compilation of all such counts per probe per sample.

We tested a 25-gene IFN-γ signature surrogate of the IFN- γ pathway activation proposed by *Sharma et al* [21]. We also tested a 12-gene chemokine-based TLS surrogate signature proposed by *Prabhakaran et al* [29]. For each surrogate signature and sample included in the analysis, enrichment scores were computed using the single sample gene set enrichment analysis (ssGSEA) tool [36] from GenePattern [37] in order to compute enrichment scores for each pairing of a sample and a gene set independent of status sample. Using this tool, gene expression values for a given sample were rank-normalized and an enrichment score was produced using the Empirical Cumulative Distribution Functions of the genes in the gene set and the remaining genes. A gene set's enrichment score represents the activity level of the biological process in which the gene set's members are coordinately up- or down-regulated.

To validate the stability of the GEP in the initial diagnosis setting, the IFN-γ and TLS surrogate signatures were computed in an independent cohort of patients suffering from oral squamous cell carcinoma (OSCC) and treated at the Groupe Hospitalier Pitié-Salpêtrière (GHPS, Paris, France) between November 2017 and August 2018. For each patient, the HTG EdgeSeq technology was used to generate targeted gene expression

profiles in per-endoscopic tumor biopsy (TB) and paired surgical specimens (SS).

### Statistical analysis

Descriptive statistics were used to summarize the baseline characteristics of the patients. Statistical analyses and plots were performed on R 4.0.0 using networkD3 v0.4 and ggplot2 v3.3.1 packages. Chi-squared or Fisher's exact test was used for statistical comparisons of categorical data. A Mann-Whitney-Wilcoxon non-parametric test was used to compare PD-L1 expression levels between two CPS groups. All statistical tests were two-sided and P values $\leqslant 0.05$ were considered to be statistically significant. For multiple testing, a false-discovery rate (FDR) was used to adjust P value.

## 3. Results

### Patient characteristics and management

Thirty-five patients with a histologically confirmed recurrent HNSCC were included. Baseline characteristics are summarized in Table 1. Median follow-up was 41 months (range 20-67) (Figure 1). Median age was 64 years (range 42–87), 71% of patients were males and 74% had a smoking history. At the time of diagnosis, the majority of tumors were locally advanced (cT3-T4 stages according to AJCC 8th edition). Twenty-two patients (44%) presented with clinical/radiological (cN+) and/or pathological (pN+) cervical lymph node involvement. Curative treatment modalities are summarized in Table 2. Ten (28%) patients had neoadjuvant chemotherapy, followed by surgery (tumor resection and/or neck dissection) for five (14%) of them. Nearly all patients (9/10, 90%) had adjuvant radiation therapy. The twenty-five patients who did not receive neoadjuvant chemotherapy were all managed with surgery followed by post-operative radiotherapy for 22/25 (88%) of them. In 55% of the patients, radiation was potentiated with chemotherapy or cetuximab. At relapse, all patients were considered as having an incurable locoregional recurrent disease. Detailed sampling information are available in supplementary Table S2.

### Temporal heterogeneity of PD-L1 expression

A majority of samples with a positive CPS using a threshold of 1 at diagnosis showed a positive CPS at relapse (19/25, 76%) while the majority of negative CPS samples at diagnosis became positive at relapse (6/8, 75%). PD-L1 status was 64% (21/33) concordant between samples at diagnosis and at relapse (Table 3 and Figure 2A).

Using a CPS threshold of 20, we found that the majority of negative CPS samples at diagnosis remained negative at relapse (17/24, 71%) and the majority of positive samples remained positive at relapse (5/9, 56%). PD-L1 status was 67% (22/33) concordant between samples at diagnosis and at relapse (Table 3 and Figure 2B).

### Correlation between PD-L1 gene expression and IHC score

A high CPS was associated with a higher PD-L1 gene level ($p$ <0.05) in initial diagnostic samples using a

CPS 1 threshold. Similarly, a high PD-L1 CPS was significantly associated with a higher PD-L1 gene level ($p < 10e-3$) in relapse samples regardless of the CPS cut-off (Figure 3).

**Temporal heterogeneity of the transcriptome**

For each sample, we used the single sample gene set enrichment analysis (ssGSEA) tool that calculates a gene set's enrichment score representing the activity level of the biological process in which the gene set's members are coordinately up- or down-regulated. Samples with a positive enrichment score were considered as 'high' and those with a negative score as 'low'. Based on the value of the enrichment score, half of the samples with a high IFN-γ signature score at diagnosis showed low scores at relapse (13/26, 50%) while the majority of samples with high scores at relapse already had high scores at diagnosis (13/15, 87%). IFN-γ signature score was 43% (15/35) concordant (Table 4 and Figure 4A).

A majority of samples with a high TLS signature score at diagnosis showed low TLS scores at relapse (11/16, 69%). Interestingly, the majority of samples with low a TLS signature score at diagnosis remained low at relapse (17/19, 90%). TLS signature score was 66% (23/35) concordant (Table 4 and Figure 4B).

**Stability of the transcriptome in the initial diagnosis setting**

In order to validate the stability of GEP in the same initial diagnosis setting, we computed the IFN-γ and TLS signature scores in the GHPS cohort of 28 per-endoscopic tumor biopsy (TB) and paired surgical resection (SR) specimens. No treatment was administered between the time of TB and SR. A total of 56 samples (paired TB and SS) from 28 patients, were profiled for gene expression using the HTG EdgeSeq technology (Table S3). One sample did not pass HTG quality control, representing an overall failure rate of 1.8% (1/56). Subsequent analysis was thus performed in 54 samples corresponding to 27 patients with paired biospecimens. There was a 78% (21/27) concordance for the IFN-γ surrogate signature and a 81% (22/27) concordance for the TLS surrogate signature between the TB and SS (Figure S3 and S4). We hypothesize that there was a high concordance rate observed in these paired specimens (TB and SS) as they were both sampled in the initial diagnosis setting, contrary to our cohort (initial diagnosis and recurrent disease), and so in line with our observations.

## 4. Discussion

In our study, PD-L1 expression demonstrated a significant temporal heterogeneity, between 33 and 36% depending on the threshold used for the CPS. In a similar manner, we observed that two GEP-based signatures (that are surrogates of the presence of TLS and IFN-γ pathway activation) are discordant in 34 to 57% of the cases between initial and recurrent lesions. In line with our observations, the GEP were stable in paired endoscopic and surgically resected specimens from the same initial diagnosis setting.

The literature is scarce on the temporal heterogeneity of the PD-L1 protein expression. Detection of PD-L1 in a 2017 study differed by 20% in primary malignant mesothelioma lesions sampled at multiple time points [38].

As previously mentioned, PD-L1 was spatially heterogeneous within a given tumor in HNSCC [12]. This seems to also be the case in other malignancies such as breast cancer [39] and non-small cell lung cancer [40]. To our knowledge, there is no data about the dynamics of PD-L1 expression between initial HNSCC and recurrent lesions.

We did not evaluate the prognostic impact of the expression of PD-L1 and GEP in initial or recurrent lesions as our cohort size was not sizeable enough to make valid interpretations.

Importantly, there was an association between high CPS and higher PD-L1 gene expression. This confirmed data of previous studies such as a large pancancer analysis in which PD-L1 gene *(CD274)* amplification was correlated with PD-L1 IHC positivity [41].

Our study has some limitations. First, around one-third of the samples analyzed were from biopsies and therefore sampling bias cannot be excluded in some specimens given the spatial heterogeneity of PD-L1. Second, concomitant treatment with irradiation at the initial stage of treatment was either chemotherapy or cetuximab, which may each harbor different effects on the expression of PD-L1 [42-44] and the gene expression profiles. For example, induction chemotherapy with docetaxel, platinum and fluorouracil (TPF) resulted in a significant increase of PD-L1 expression in locally advanced HNSCC patients [44]. The effect of cetuximab on the expression of PD-L1 in HNSCC is less known. Jie et al. found that the increased frequency of PD-1+ and TIM+ infiltrating lymphocytes (TILs) during cetuximab treatment inversely correlated with objective response [45].

In conclusion, PD-L1 expression and GEP in HNSCC show a marked temporal discordance, which should be taken into consideration as they are used and developed as predictive biomarkers for ICI. Since our work is retrospective in nature with a relatively small number of patients, larger prospective studies are needed to confirm our conclusions about this temporal heterogeneity and to better assess the impact of chemotherapy/cetuximab on the expression of PD-L1 and the dynamics of the transcriptome.

## Author contributions

Conceptualization: AK, JF and JB; Data curation: AK, JB, LM, NB, CC, VA and JAP; Formal analysis: AK, JB, LM, JAP and PS; Funding acquisition: PS, PZ and JF; Investigation: AK, JB, LM, CC, NB, JAP, PS and NG ; Methodology: AK, NB, MK, VA, JF and PS; Project administration: PS, CLT, MK and JF; Resources: NB, PZ, JF, CLT, MK and PS; Software: LM, VA and JB; Supervision: PS, JF and CLT; Validation: PS, JF and CLT; Visualization: MK, PZ, MK and LM; Roles/Writing - original draft: AK and JB; Writing - review & editing: AK, JB and PS.

## Acknowledgments

The authors thank the local Biological Resources Center (BB-0033-00050, CRB Centre Léon Bérard, Lyon France) and Centre de Ressources Biologiques des Hospices Civils de Lyon (BB-0033-00046) for their help in this study.

## FIGURE CAPTIONS

**Figure 1. Cohort follow-up (n=35) from the first surgery/biopsy to the last follow-up date.**

**Figure 2A**. **Comparison of PD-L1 expression between initial and recurrent lesions.**

PD-L1 was evaluated with immunohistochemistry (IHC) using the Combined Positive Score (CPS) with a positivity threshold of 1. PD-L1 status was 64% concordant (21/33) between initial and recurrent lesions.

**Figure 2B**. **Comparison of PD-L1 expression between initial and recurrent lesions.**

PD-L1 was evaluated with immunohistochemistry (IHC) using the Combined Positive Score (CPS) with a positivity threshold of 20. PD-L1 status was 67% concordant (22/33) between initial and recurrent lesions.

**Figure 3. Correlation between PD-L1 gene expression and Immunohistochemistry (IHC) score.**

A high PD-L1 gene expression level correlated significantly with a higher CPS score (p-value ranging from 0.05-0.1) in initial diagnostic samples using a $\geq 1$ CPS cut-off.

A high PD-L1 gene expression level correlated significantly with a higher CPS score ($p < 10e-3$) in relapse samples regardless of the CPS cut-off.

"***" for p-value < 10e-3;

"•" for p-value ranging from 0.05-0.1

"NS" for p-value > 0.1

**Figure 4A. Evolution of the transcriptomic Interferon-gamma signature (*Sharma et al.2017*).**

IFN-γ signature was 43% (15/35) concordant between initial and recurrent lesions.

**Figure 4B. Evolution of the Tertiary Lymphoid Structure (TLS) signature (*Prabhakaran et al.2017*).**

TLS signature was 66% (23/35) concordant between initial and recurrent lesions.

371

**Table 1. Baseline characteristics (n = 35)**

| Variables | Overall population | |
|---|---|---|
| Age (Median, range) | 64 | 42-87 |
| **Gender** (N, %) | | |
| Male | 25 | 71% |
| Female | 10 | 29% |
| **Smoking history (N, %)** | | |
| Current/Former | 26 | 74% |
| No | 9 | 26% |
| **Sample type (N, %)** | | |
| Biopsy | 11 | 31% |
| Surgical | 24 | 69% |
| **Disease site (N, %)** | | |
| Oral cavity | 15 | 43% |
| Oropharynx | 13 | 37% |
| Hypopharynx | 4 | 11% |
| Larynx | 2 | 6% |
| Maxillary Sinus | 1 | 3% |
| **HPV status (N, %)** | | |
| Negative | 16 | 46% |
| Positive | 7 | 20% |
| Unknown | 12 | 34% |

| | | |
|---|---|---|
| **T stage according to AJCC 8th edition (N, %)** | | |
| T1 | 2 | 6% |
| T2 | 12 | 34% |
| T3 | 7 | 20% |
| T4 | 12 | 34% |
| Non evaluable | 2 | 6% |
| **N stage according to AJCC 8th edition (N, %)** | | |
| N0 | 11 | 31% |
| N1 | 4 | 11% |
| N2 | 17 | 49% |
| N3 | 1 | 3% |
| Missing data | 2 | 6% |

**Table 2. Curative treatment modality (n=35)**

| | | |
|---|---|---|
| **Neoadjuvant chemotherapy (N, %)** | | |
| No | 23 | 66% |
| Yes | 10 | 29% |
| Missing data | 2 | 6% |
| **Tumor resection (N, %)** | | |
| No | 8 | 23% |
| Yes | 25 | 71% |
| Missing data | 2 | 6% |
| **Neck dissection (N, %)** | | |
| No | 8 | 23% |
| Yes | 25 | 71% |
| Missing data | 2 | 6% |
| **Radiation therapy (N, %)** | | |
| No | 4 | 11% |
| Yes | 31 | 89% |
| **Concomitant systemic therapy (N, %)** | | |
| Chemotherapy | 12 | 39% |
| Cetuximab | 5 | 16% |
| No | 14 | 45% |

**Table 3. PD-L1 Combined Positive Score (CPS) in all samples (n = 33)**

| | Status at diagnosis | Status at relapse | Number (N, %) |
|---|---|---|---|
| PDL1 CPS ≥ 1 | Positive | Positive | 19 (58) |
| | Negative | Positive | 6 (18) |
| | Positive | Negative | 6 (18) |
| | Negative | Negative | 2 (6) |
| PDL1 CPS ≥ 20 | Positive | Positive | 5 (15) |
| | Negative | Positive | 7 (21) |
| | Positive | Negative | 4 (12) |
| | Negative | Negative | 17 (52) |

**Table 4. Interferon-gamma (IFN-γ) and tertiary lymphoid structure (TLS) signature enrichment scores in all samples (n = 35)**

| | Enrichment score at diagnosis | Enrichement score at relapse | Number (N, %) |
|---|---|---|---|
| IFN-γ signature | High | High | 13 (37) |
| | Low | High | 2 (6) |
| | High | Low | 13 (37) |
| | Low | Low | 7 (20) |
| TLS signature | High | High | 5 (14) |
| | Low | High | 2 (6) |
| | High | Low | 11 (31) |
| | Low | Low | 17 (49) |

## References


1. Bray F, Ferlay J, Soerjomataram I, Siegel RL, Torre LA, Jemal A. Global cancer statistics 2018: GLOBOCAN estimates of incidence and mortality worldwide for 36 cancers in 185 countries. *CA Cancer J Clin*. 2018 Nov;68(6):394-424. doi: 10.3322/caac.21492.

2. Karabajakian A, Toussaint P, Neidhardt EM, Paulus V, Saintigny P, Fayette J. Chemotherapy for recurrent/metastatic head and neck cancers. *Anticancer Drugs* 2017;28:357-61. doi: 10.1097/CAD.0000000000000473.

3. Ferris RL, Blumenschein G Jr, Fayette J, Guigay J, Colevas AD, Licitra L, et al. Nivolumab for Recurrent Squamous-Cell Carcinoma of the Head and Neck. *N Engl J Med.* 2016 Nov 10;375(19):1856-1867. doi: 10.1056/NEJMoa1602252.

4. Ferris, Robert L, George Blumenschein, Jerome Fayette, Guigay J, Colevas AD, Licitra L, et al. Nivolumab vs investigator's choice in recurrent or metastatic squamous cell carcinoma of the head and neck: 2-year long-term survival update of CheckMate 141 with analyses by tumor PD-L1 expression. *Oral Oncol.* 2018 Jun;81:45-51. doi: 10.1016/j.oraloncology.2018.04.008.

5. Cohen EEW, Soulières D, Le Tourneau C, Dinis J, Licitra L, Ahn MJ, et al. Pembrolizumab versus methotrexate, docetaxel, or cetuximab for recurrent or metastatic head-and-neck squamous cell carcinoma (KEYNOTE-040): a randomised, open-label, phase 3 study. *Lancet*. 2019 Jan 12;393(10167):156-167. doi: 10.1016/S0140-6736(18)31999-8.

6. Burtness B, Harrington KJ, Greil R, Soulières D, Tahara M, de Castro G Jr, et al. Pembrolizumab alone or with chemotherapy versus cetuximab with chemotherapy for recurrent or metastatic squamous cell

carcinoma of the head and neck (KEYNOTE-048): a randomised, open-label, phase 3 study. *Lancet.* 2019 Nov 23;394(10212):1915-1928. doi: 10.1016/S0140-6736(19)32591-7.

7. Oliva M, Spreafico A, Taberna M, Alemany L, Coburn B, Mesia R, et al. Immune biomarkers of response to immune-checkpoint inhibitors in head and neck squamous cell carcinoma. *Ann Oncol*. 2019 Jan 1;30(1):57-67. doi: 10.1093/annonc/mdy507.

9. Saâda-Bouzid E, Defaucheux C, Karabajakian A, Coloma VP, Servois V, Paoletti X, et al. Hyperprogression during anti-PD-1/PD-L1 therapy in patients with recurrent and/or metastatic head and neck squamous cell carcinoma. *Ann Oncol*. 2017 Jul 1;28(7):1605-1611. doi:10.1093/annonc/mdx178.

10. Karabajakian A, Garrivier T, Crozes C, Gadot N, Blay JY, Bérard F, et al. Hyperprogression and impact of tumor growth kinetics after PD1/PDL1 inhibition in head & neck squamous cell carcinoma. *Oncotarget* 2020 May 5;11(18):1618-1628. doi: 10.18632/oncotarget.27563.

11. Philip R, Carrington L, Chan M. US FDA perspective on challenges in co-developing in vitro companion diagnostics and targeted cancer therapeutics. *Bioanalysis* 2011; 3(4): 383–389. doi: 10.4155/bio.11.1.

12. McLaughlin, J., Han, G., Schalper, K. A, Carvajal-Hausdorf D, Pelekanou V, Rehman J, et al. Quantitative assessment of the heterogeneity of PD-L1 expression in non-small-cell lung cancer. *JAMA Oncol*. 2, 46–54 (2016). doi: 10.1001/jamaoncol.2015.3638.

13. Rasmussen JH, Lelkaitis G, Håkansson K, Vogelius IR, Johannesen HH, Fischeret BM, et al. Intratumor heterogeneity of PD-L1 expression in head and neck squamous cell carcinoma. *Br J Cancer*. 2019 May;120(10):1003-1006. doi: 10.1038/s41416-019-0449-y.

14. Cimino-Mathews A, Thompson E, Taube JM, Ye X, Lu Y, Meekeret A, et al. PD-L1 (B7-H1)

456 expression and the immune tumor microenvironment in primary and metastatic breast carcinomas. *Hum*
457 *Pathol* 2016; 47(1): 52–63. doi: 10.1016/j.humpath.2015.09.003.
458
459 15. Gadiot J, Hooijkaas AI, Kaiser ADM, van Tinteren H, van Boven H, Blank C. Overall survival and PD-
460 L1 expression in metastasized malignant melanoma. *Cancer* 2011; 117(10): 2192–2201. doi:
461 10.1002/cncr.25747.
462
463 16. Hanna GJ, Lizotte P, Cavanaugh, Kuo FC, Shivdasani P, Frieden A, Chau NG, et al. Frameshift events
464 predict anti- PD-1/L1 response in head and neck cancer. *JCI Insight* 2018; 3(4): e98811. doi:
465 10.1172/jci.insight.98811.
466
467 17. Seiwert T, Haddad R, Bauml J, Weiss J, Pfister DG, Gupta S, et al. Biomarkers predictive of response to
468 pembrolizumab in head and neck cancer (HNSCC). *AACR meeting* 2018. Abstract 339.
469
470 18. Ortiz-Cuaran S, Bouaoud J, Karabajakian A, Fayette J, Saintigny P. Precision Medicine Approaches to
471 Overcome Resistance to Therapy in Head and Neck Cancers. *Front Oncol*. 2021 Feb 25;11:614332. doi:
472 10.3389/fonc.2021.614332.
473
474 19. Serafini MS, Lopez-Perez L, Fico G, Licitra L, De Cecco L, Resteghini C. Transcriptomics and
475 Epigenomics in head and neck cancer: available repositories and molecular signatures. *Cancers Head Neck*.
476 2020 Jan 21;5:2. doi: 10.1186/s41199-020-0047-y.
477
478 20. Zaretsky JM, Garcia-Diaz A, Shin DS, et al. Mutations associated with acquired resistance to PD-1
479 blockade in melanoma. *N Engl J Med* 2016; 375: 819–29. doi: 10.1056/NEJMoa1604958.
480
481 21. Gao J, Shi LZ, Zhao H, et al. Loss of IFN-γ signaling in tumor cells as a mechanism of primary
482 resistance to anti-CTLA-4 therapy. *Cell*. 2016; 167: 397–404. doi: 10.1080/1744666X.2021.1847644.
483
484 22. Sharma P, Retz M, Siefker-Radtke A, Baron A, Necchi A, Bedke J, et al. Nivolumab in metastatic

urothelial carcinoma after platinum therapy (CheckMate 275): a multicentre, single-arm, phase 2 trial. *Lancet Oncol.* 2017 Mar;18(3):312-322. doi: 10.1016/S1470-2045(17)30065-7.

23. Fehrenbacher, L., A. Spira, M. Ballinger, M. Kowanetz, J. Vansteenkiste, J. Mazieres, K. Park, et al. Atezolizumab versus docetaxel for patients with previously treated non-small-cell lung cancer (POPLAR): a multicentre, open-label, phase 2 randomised controlled trial. *Lancet* 2016 Apr 30;387(10030):1837-46. doi: 10.1016/S0140-6736(16)00587-0.

24. Haddad RI, Seiwert TY, Chow LQM, Gupta S, Weiss J, Gluck I, et al. Genomic determinants of response to pembrolizumab in head and neck squamous cell carcinoma (HNSCC). *J Clin Oncol* 2017; 35(Suppl 15): 6009.

25. Cristescu R, Mogg R, Ayers M, Albright A, Murphy E, Yearley J, et al. Pan-tumor genomic biomarkers for PD-1 checkpoint blockade-based immunotherapy. *Science*. 2018 Oct 12;362(6411):eaar3593. doi: 10.1126/science.aar3593.

26. Sautès-Fridman C, Petitprez F, Calderaro J, Fridman WH. Tertiary lymphoid structures in the era of cancer immunotherapy. *Nat Rev Cancer*. 2019 Jun;19(6):307-325. doi: 10.1038/s41568-019-0144-6.

27. Cottrell TR, Thompson ED, Forde PM, Stein JE, Duffield AS, Anagnostou V, et al. Pathologic features of response to neoadjuvant anti-PD-1 in resected non-small-cell lung carcinoma: a proposal for quantitative immune-related pathologic response criteria (irPRC). *Ann Oncol*. 2018 Aug 1;29(8):1853-1860. doi: 10.1093/annonc/mdy218.

28. Maldonado L,vTeague JE, Morrow MP, Jotova I, Wu TC, Wang C, et al. Intramuscular therapeutic vaccination targeting HPV16 induces T cell responses that localize in mucosal lesions. *Sci Transl Med*. 2014 Jan 29;6(221):221ra13. doi: 10.1126/scitranslmed.3007323.

29. Coppola D, Nebozhyn M, Khalil F, Dai H, Yeatman T, Loboda A, et al. Unique ectopic lymph node-like structures present in human primary colorectal carcinoma are identified by immune gene array profiling. *Am J Pathol* . 2011 Jul;179(1):37-45. doi: 10.1016/j.ajpath.2011.03.007.

30. Prabhakaran S, Rizk VT, Ma Z, Cheng C-H, Berglund AE, Coppola D, et al. Evaluation of invasive breast cancer samples using a 12-chemokine gene expression score: correlation with clinical outcomes. *Breast Cancer Res* . 2017 Jun 19;19(1):71. doi: 10.1186/s13058-017-0864-z.

31. Hennequin A, Derangère V, Boidot R, Apetoh L, Vincent J, Orry D, et al. Tumor infiltration by Tbet+

effector T cells and CD20+ B cells is associated with survival in gastric cancer patients. *Oncoimmunology.* 2015 Jun 3;5(2):e1054598. doi: 10.1080/2162402X.2015.1054598.

32. Gu-Trantien C, Loi S, Garaud S, Equeter C, Libin M, de Wind A, et al. $CD4^+$ follicular helper T cell infiltration predicts breast cancer survival. *J Clin Invest*. 2013 Jul;123(7):2873-92. doi: 10.1172/JCI67428.

33. Brandone N, Mascaux C, Caselles K, Rouquette I, Lantuejoul S, Garcia S. Validation of the QR1 Antibody for the Evaluation of PD-L1 Expression in Non-Small Cell Lung Adenocarcinomas. Appl *Immunohistochem Mol Morphol*. 2020 Jan;28(1):23-29. doi: 10.1097/PAI.0000000000000758.

34. Lantuejoul S, Sound-Tsao M, Cooper WA, Girard N, Hirsch FR, Roden AC, et al. PD-L1 Testing for Lung Cancer in 2019: Perspective From the IASLC Pathology Committee. *J Thorac Oncol*. 2020 Apr;15(4):499-519. doi: 10.1016/j.jtho.2019.12.107.

35. O'Rourke D, Sanchez-Garcia JF, Rolfe PA, Huang A, Wang D, Scheuenpflug J, et al. Abstract 2016: Comparison of HTG-edge targeted RNA sequencing platform with whole transcriptome RNA sequencing for clinical biomarker studies. *AACR Annual Meeting 2020.*

36. Subramanian A, Tamayo P, Mootha VK, Mukherjee S, Ebert BL, Gillette MA, Paulovich A, et al. Gene set enrichment analysis: a knowledge-based approach for interpreting genome-wide expression profiles. *Proc Natl Acad Sci U S A* 2005; 102: 15545-15550. doi: 10.1073/pnas.0506580102.

37. Reich M, Liefeld T, Gould J, Lerner J, Tamayo P, Mesirov JP. GenePattern 2.0. *Nat Genet* 2006; 38: 500-501. doi: 10.1038/ng0506-500.

38. Terra SBSP, Mansfield AS, Dong H, Peikert T, Roden AC. Temporal and spatial heterogeneity of programmed cell death 1-Ligand 1 expression in malignant mesothelioma. *Oncoimmunology.* 2017 Jul 27;6(11):e1356146. doi: 10.1080/2162402X.2017.1356146.

39. Stovgaard ES, Bokharaey M, List-Jensen K, Roslind A, K€umler I, Høgdall E, et al. PD-L1 diagnostics in the neoadjuvant setting: implications of intratumoral heterogeneity of PD-L1 expression in triple negative breast cancer for assessment in small biopsies. *Breast Cancer Res Treat* 2020;181:553–60. doi: 10.1007/s10549-020-05655-w.

40. Haragan A, Field JK, Davies MPA, Escriu C, Gruver A, Gosney JR. Heterogeneity of PD-L1 expression in non-small cell lung cancer: Implications for specimen sampling in predicting treatment response. *Lung Cancer* 2019;134: 79–84. doi: 10.1016/j.lungcan.2019.06.005.

41. Huang RSP, Haberberger J, Severson E, DL, Hemmerich A, Edgerly C, et al. A pan-cancer analysis of PD-L1 immunohistochemistry and gene amplification, tumor mutation burden and microsatellite instability in 48,782 cases. *Mod Pathol*. 2020 Sep 3. doi: 10.1038/s41379-020-00664-y.

42. Fournel L, Wu Z, Stadler N, Damotte D, Lococo F, Boulle G, et al. Cisplatin increases PD-L1 expression and optimizes immune check-point blockade in non-small cell lung cancer. *Cancer Lett* 2019;464:5–14. doi: 10.1016/j.canlet.2019.08.005.

43. Park S, Joung J-G, Min YW, Nam J-Y, Ryu D, Oh D, et al. Paired whole exome and transcriptome analyses for the Immunogenomic changes during concurrent chemoradiotherapy in esophageal squamous cell carcinoma. *J Immunother Cancer* 2019;7:128.37. doi: 10.1186/s40425-019-0609-x.

44. Leduc C, Adam J, Louvet E, Sourisseau T, Dorvault N, Bernard M, et al. TPF induction chemotherapy increases PD-L1 expression in tumour cells and immune cells in head and neck squamous cell carcinoma. *ESMO Open*. 2018;3(1):e000257. doi: 10.1136/esmoopen-2017-000257.

45. Jie H-B, Srivastava RM, Argiris A, Bauman JE, Kane LP, Ferris RL. Increased PD-1 + and TIM-3 + TILs during Cetuximab Therapy Inversely Correlate with Response in Head and Neck Cancer Patients. *Cancer Immunol Res*. 2017 May;5(5):408-416. doi: 10.1158/2326-6066.CIR-16-0333.

**Declaration of interest**

PS is a member of HTG Diagnostics Scientific Advisory Board and receives research grants from HTG Diagnostics, Inivata, ArcherDx, Bristol-Myers Squibb, Roche Molecular Diagnostics, Roche, AstraZeneca, Novartis, Bristol-Myers Squibb Foundation and Illumina. JF reports grants, personal fees and non-financial support from Bristol-Myers Squibb, personal fees and non-financial support from MSD, personal fees from Merck, personal fees and non-financial support from Astrazeneca, personal fees from Rakuten, personal fees from Biogen and personal fees from Innate Pharma. CLT participated in advisory boards from BMS, MSD, Merck Serono, Roche, Nanobiotix, Rakuten, Seattle Genetics, Rakuten, Astra Zeneca, GSK, Celgene.

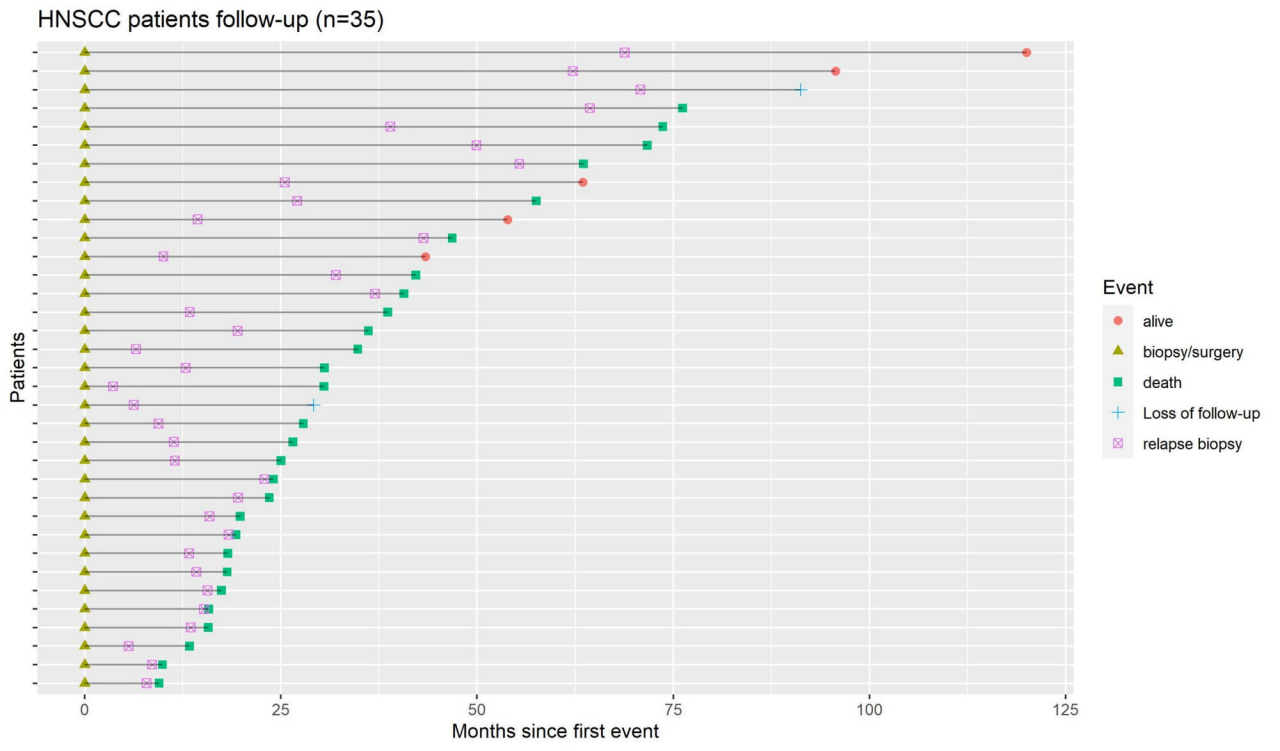
HNSCC patients follow-up (n=35)
Patients
Months since first event
0
25
50
75
100
125
Event
alive
biopsy/surgery
death
Loss of follow-up
relapse biopsy

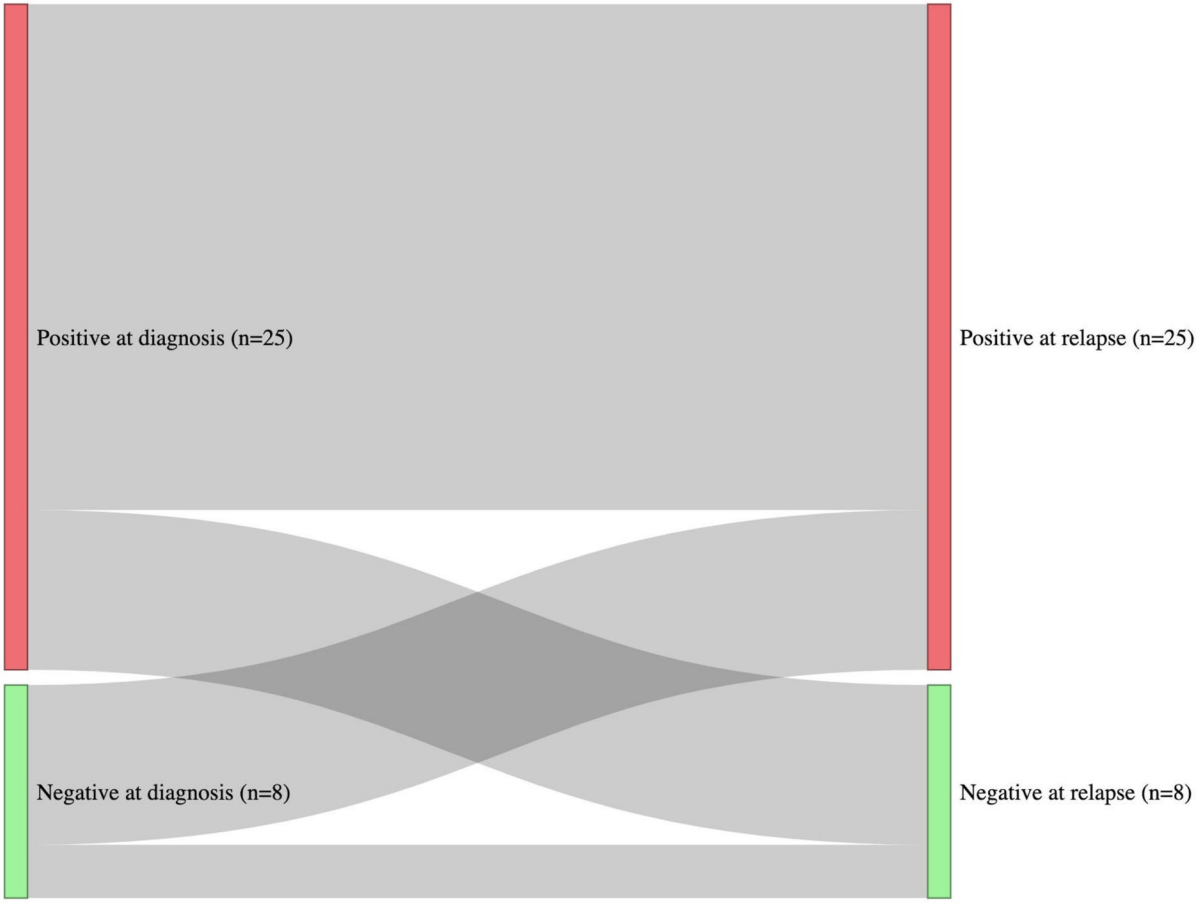
Positive at diagnosis (n=25)
Negative at diagnosis (n=8)
Positive at relapse (n=25)
Negative at relapse (n=8)

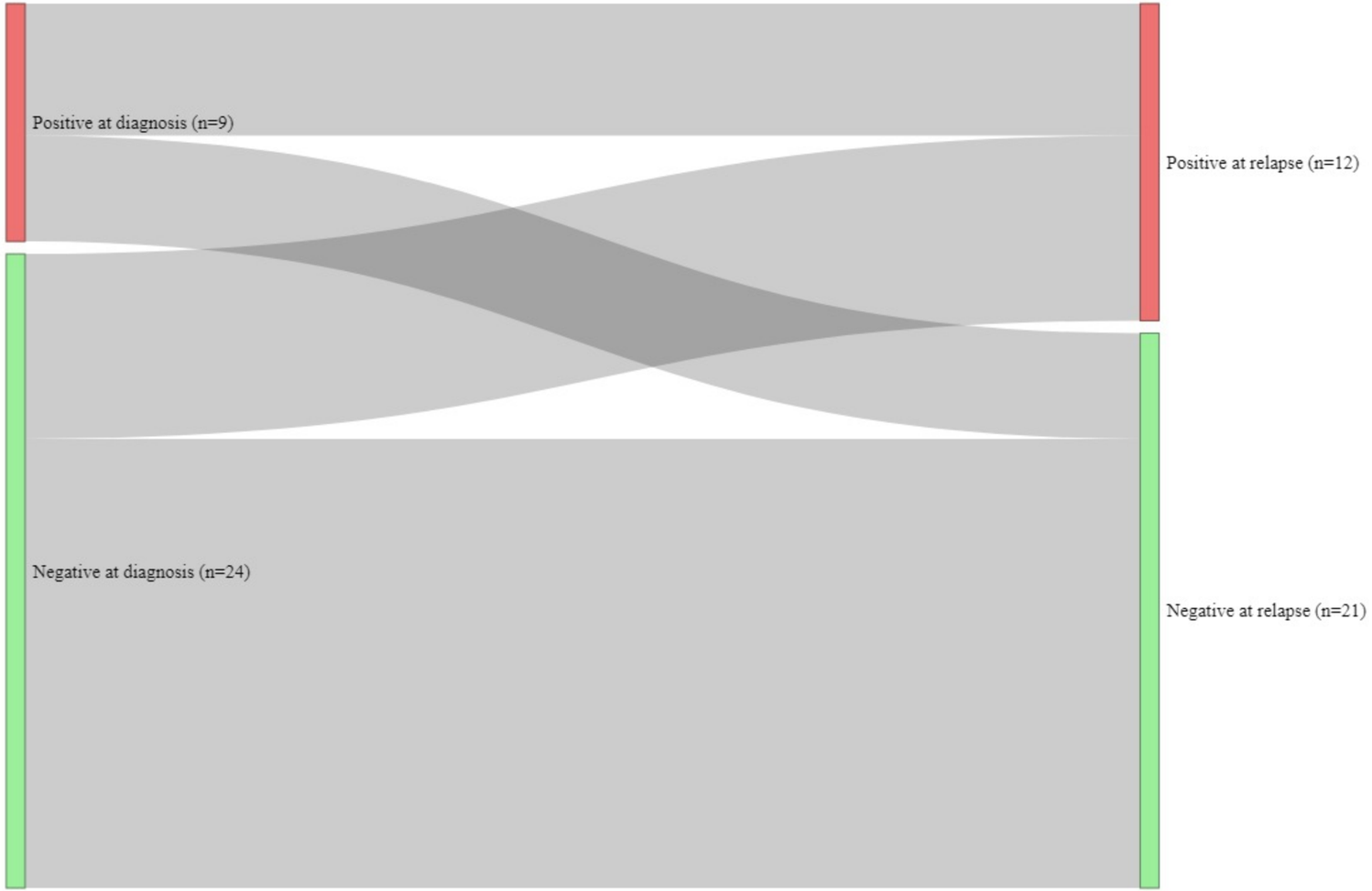
Positive at diagnosis (n=9)
Negative at diagnosis (n=24)
Positive at relapse (n=12)
Negative at relapse (n=21)

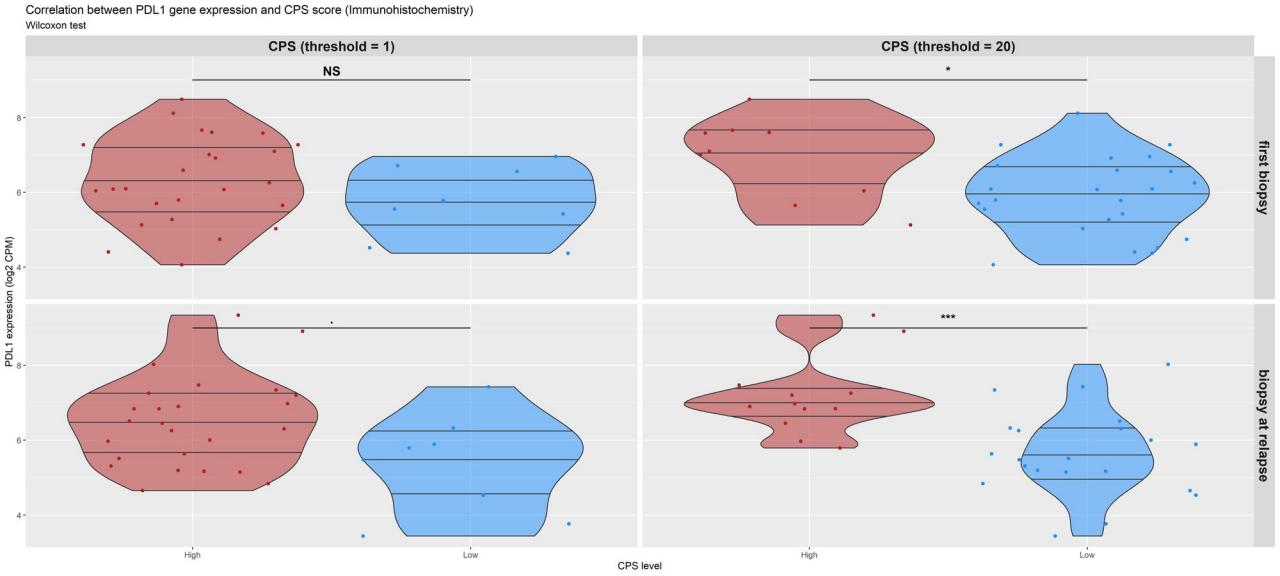
Correlation between PDL1 gene expression and CPS score (Immunohistochemistry)
Wilcoxon test
CPS (threshold = 1)
CPS (threshold = 20)
NS
*
.
***
first biopsy
biopsy at relapse
PDL1 expression (log2 CPM)
8
6
4
High
Low
CPS level

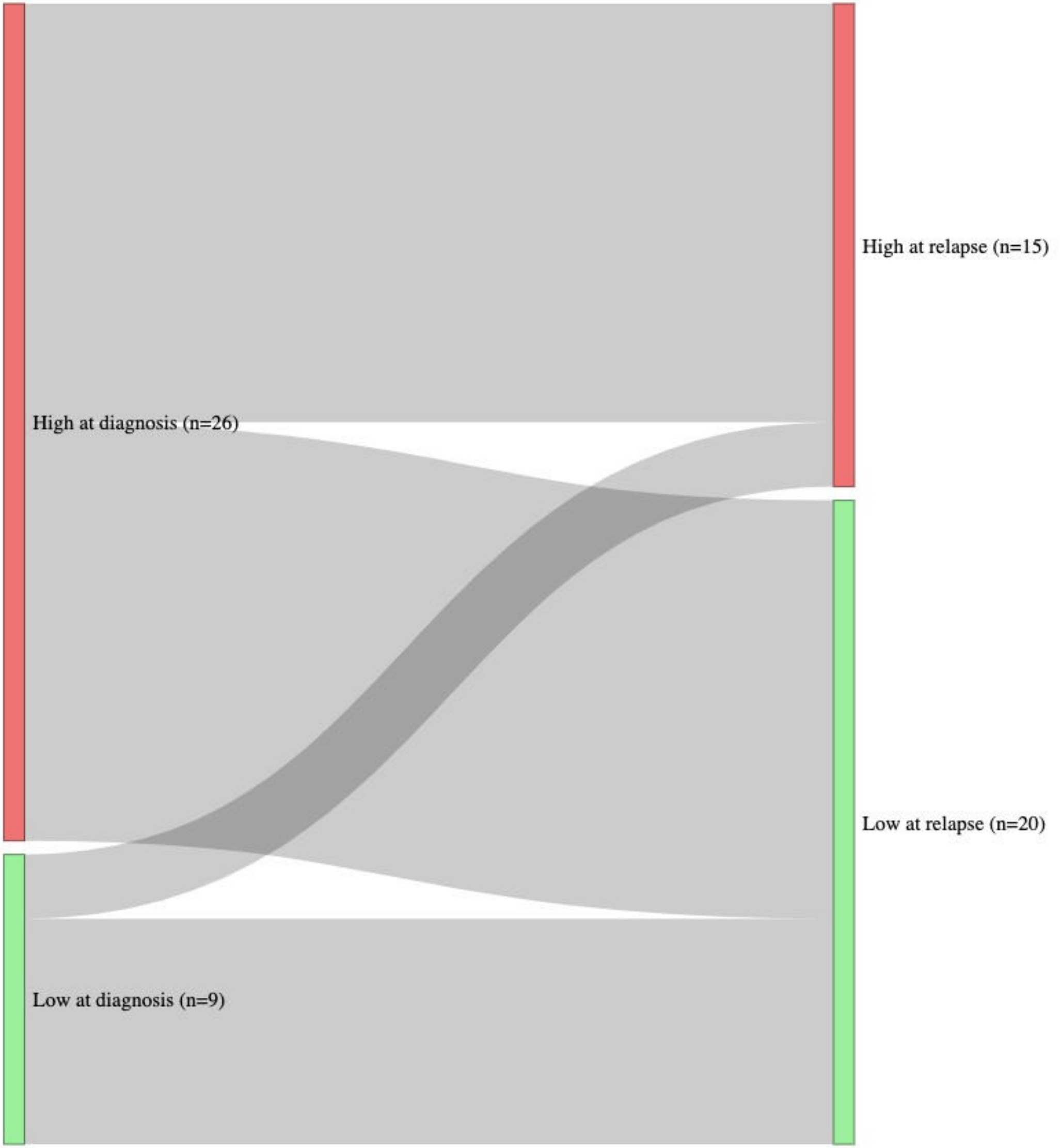
High at diagnosis (n=26)
Low at diagnosis (n=9)
High at relapse (n=15)
Low at relapse (n=20)

High at diagnosis (n=16)

Low at diagnosis (n=19)

High at relapse (n=7)

Low at relapse (n=28)